Published in final edited form as:
Circulation. 2010 September 14; 122(11 Suppl): S124–S131. doi:10.1161/CIRCULATIONAHA.109.928424.

MicroRNA-210 as a Novel Therapy for Treatment of Ischemic Heart Disease

Shijun Hu, PhD[1,2], **Mei Huang, PhD**[1,2], **Zongjin Li, PhD**[1,2], **Fangjun Jia, PhD**[1,2], **Zhumur Ghosh, PhD**[1,2], **Maarten A. Lijkwan, MD**[3], **Pasquale Fasanaro, PhD**[4], **Ning Sun, PhD**[1,2], **Xi Wang, MD, PhD**[3], **Fabio Martelli, PhD**[5], **Robert C. Robbins, MD**[3], and **Joseph C. Wu, MD, PhD**[1,2]

[1]Department of Medicine, Division of Cardiology, Stanford, CA, USA

[2]Department of Radiology, Molecular Imaging Program, Stanford, CA, USA

[3]Department of Cardiothoracic Surgery, Stanford, CA, USA

[4]IRCCS-Policlinico San Donato, Milan, Italy

[5]Istituto Dermopatico dell'Immacolata-IRCCS, Rome, Italy

Abstract

Background—MiRNAs are involved in various critical functions, including the regulation of cellular differentiation, proliferation, angiogenesis, and apoptosis. Here we hypothesize that miR-210 can rescue cardiac function after myocardial infarction by up-regulation of angiogenesis and inhibition of cellular apoptosis in the heart.

Methods and Results—Using miRNA microarrays, we first showed that miR-210 was highly expressed in live mouse HL-1 cardiomyocytes compared with apoptotic cells after 48 hours of hypoxia exposure. We confirmed by PCR that miR-210 was robustly induced in these cells. Gain-of-function and loss-of-function approaches were used to investigate miR-210 therapeutic potential *in vitro*. Following transduction, miR-210 can upregulate several angiogenic factors, inhibit caspase activity, and prevent cell apoptosis compared with control. Afterwards, adult FVB mice underwent intramyocardial injections with minicircle (MC) vector carrying miR-210 precursor (MC-210), minicircle carrying miR-scramble (MC-Scr), or sham surgery. At 8 weeks, echocardiography showed a significant improvement of left ventricular fractional shortening (FS) in the MC-210 group compared to MC-Scr control. Histological analysis confirmed decreased cellular apoptosis and increased neovascularization. Finally, two potential targets of miR-210, Efna3 and Ptp1b, involved in angiogenesis and apoptosis were confirmed via additional experimental validation.

Conclusion—miR-210 can improve angiogenesis, inhibit apoptosis, and improve cardiac function in a murine model of myocardial infarction. It represents a potential novel therapeutic approach for treatment of ischemic heart disease.

Correspondence: Joseph C. Wu, MD, PhD Stanford University School of Medicine, Grant Building S140, Stanford, CA 94305-5111, Ph: 650-736-2246, Fax: 650-736-0234, joewu@stanford.edu.

Journal Subject Codes: [88] Gene therapy

Conflict of Interest Disclosures: None

Keywords

microRNA; minicircle vector; gene therapy; ischemic heart disease

INTRODUCTION

Ischemic heart disease (IHD) is the number one cause of morbidity and mortality in the US owing to aging, obesity, diabetes, and other co-morbid diseases. One potent therapeutic approach for IHD is to reduce oxygen consumption, inhibit cardiomyocyte apoptosis, increase coronary flow, and induce revascularization. MicroRNAs (miRNAs), representing ~1% the eukaryotic transcriptome, is an evolutionarily conserved family of non-coding RNAs of 20–22 nucleotides that negatively regulate the expression of protein-coding genes through translational inhibition and RNA decay. miRNAs are involved in diverse biological progresses, including cellular differentiation, proliferation, angiogenesis, and apoptosis1. To date, 721 miRNAs have been discovered in human and 597 miRNAs in mouse according to the miRBase Sequence Database Release 14 (http://www.mirbase.org/). miRNAs can regulate approximately 30% human protein-coding genes2. Importantly, the successful suppression of murine liver cancer by systemic delivery of miR-26a suggests the potential of utilizing miRNAs as a novel therapeutic tool.3

In the cardiovascular field, miRNAs have also been implicated as a significant factor in various physiological and pathological diseases.4 For example, miR-21 expression is significantly down-regulated in infarcted heart but up-regulated in border areas, hence serving a possible protective role in the early phase of acute myocardial infarction.5 Recently, several groups have reported miR-210 as one of several hypoxia-induced miRNAs critical for cell survival and angiogenesis.6 Huang et al. demonstrated that miR-210 is HIF-1α dependent and provided further insight into its functional role during tumor initiation.7 They showed that increasing miR-210 expression gives the tumor cells an opportunity to prevail under initial stressful conditions.

In this study, we hypothesize that miRNA may play a significant role in regulating angiogenesis and apoptosis after myocardial infarction. We demonstrate for the first time that delivery of miR-210 through a non-viral minicircle vector in the ischemic heart can improve heart function by promoting angiogenesis and inhibiting apoptosis. Our results show miR-210 may lead to a novel therapy for ischemic heart disease.

MATERIALS AND METHODS

Cell culture, cell transduction, and hypoxic conditions

293FT cells (Invitrogen) were used to generate recombinant replication-deficient lentivirus used for *in vitro* assays as described.8 Mouse HL-1 cardiomyocytes were cultured in Claycomb media supplement 10% fetal bovine serum (Sigma), 0.1 M norepinephrine (Sigma), 2 mM L-glutamine (Invitrogen), and penicillin/streptomycin (Invitrogen) in a humidified 5% CO2 incubator at 37°C. Hypoxia was achieved by placing cells in a hypoxia chamber filled with 5% CO_2, 1% O_2, and 94% N_2 at 37°C. At different time points during hypoxic treatment, cells were harvested for analysis of miR-210 levels. Angiogenesis factor antibody array (Panomics Inc., Fremont, CA) was used to investigate the angiogenic potential of miR-210. Apoptosis assays were performed after 48 hours of transduction with lentivirus carrying miR-210 precursor (Pre-210), lentivirus carrying miR-scramble (Pre-Scr), lentivirus carrying anti-sense of miR-210 (Anti-210), and lentivirus carrying anti-sense of miR-scramble (Anti-Scr) using a Caspase-Glo 3/7 Assay (Promega) according to

manufacturer's instructions. The caspase activities for all samples were normalized to that of an equal protein amount. The data obtained are from experiments performed in triplicate.

MicroRNA microarray and data analysis

Microarray assay was performed using a service provider (LC Sciences, Houston, TX). The assay started with 4 μg total RNA sample. Small RNAs were isolated with a poly(A) tail using poly(A) polymerase. Hybridization was performed overnight on a microfluidic chip consisting of chemically modified nucleotide coding segment complementary to target microRNA (miRBase 13.0) or other control RNA. Fluorescence images were collected using a laser scanner and digitized using Array-Pro image analysis software. Raw data matrix is then subtracted by the background matrix. Data adjustment includes data filtering, Log2 transformation, gene centering, and normalization. 2-sample t-test was conducted for statistical analysis.

Preparation of minicircle DNA

Minicircles are the product of site-specific intramolecular recombination between the attB and attP sites driven by bacteriophage ΦC31 integrase (Supplemental Figure 1). The DNA fragment containing firefly luciferase and enhanced *g*reen fluorescent protein (MC-LG), mir-210 precursor (MC-210), or miR-scramble (MC-Scr) were bluntly ligated between attB and attP sites of p2øC31 minicircle plasmid. The minicircle DNA plasmid (gift from Dr. Mark Kay, Stanford) was produced as described previously.9 Briefly, E. coli Top10 (Invitrogen) was transformed by parental plasmids. A single colony of the transformants was grown at 37°C overnight. Then 800 ml of bacterial culture was spun down in a centrifuge at 1500g for 15 min at RT. The pellet was resuspended with 200 ml of fresh LB broth (pH 7.0) containing 1% L-(+)-arabinose. The resuspended bacteria were incubated at 30°C at 250 rpm for 2 hour. Subsequently, 300 ml of fresh LB broth (pH 8.0) containing 1% L-(+)-arabinose was added and the bacteria were incubated for additional 2 hour at 37°C. Minicircle DNA was isolated using plasmid purification kits from Qiagen (Valencia, CA).

Surgical model of mouse myocardial infarction (MI)

Adult female FVB mice (10 weeks old) were purchased from Charles River Laboratories (Wilmington, MA). Ligation of the mid left anterior descending (LAD) artery was performed by a single experienced microsurgeon (XW). Myocardial infarction was confirmed by myocardial blanching and EKG changes. After 15 min, the animals were then injected intramyocardially with 25 μg of minicircles carrying miR-210 precursor (MC-210), or minicircles carrying Scramble (MC-Scr) (n=15 per group). Injections were made near the peri-infarct region at 3 different sites with a total volume of 25 μl using a 29-gauge Hamilton syringe. The third group was performed sham, which underwent surgery but not LAD ligation (n=15). Study protocols were approved by the Stanford Animal Research Committee.

Echocardiographic analysis of left ventricular function

Echocardiography was performed before (day -7) and after (week 2, week 4, and week 8) the LAD ligation. A Siemens-Acuson Sequioa C512 system equipped with a multi-frequency (8–14 MHZ) 15L8 transducer was used by an investigator (MH) blinded to group designation. Analysis of the M-mode images was performed using DicomWorks 1.3.5 (http://dicom.online.fr) analysis software. Left ventricular end-diastolic diameter (EDD) and end-systolic diameter (ESD) were measured and used to calculate left ventricular fractional shortening (FS) by the following formula: FS = (EDD − ESD)/EDD.

Pressure-volume loop measurement

Invasive steady-state hemodynamic measurements were performed (n = 5 mice per group for MC-210, MC-Scr, and sham) at week 4 as described previously.10 Briefly, after midline neck incision, a 1.4F conductance catheter (Millar Instruments, Houston, Texas) was introduced into the left ventricle through the right carotid artery. The signals were continuously recorded using PV conductance system coupled to a PowerLab/4SP analog to digital converter (AD Instruments, Colorado Springs, Colorado). Data were analyzed by using a cardiac PV analysis program (PVAN 3.4, Millar Instruments) and Chart/Scope Software (AD Instruments).

In vivo optical bioluminescence imaging (BLI)

BLI was performed using the IVIS Spectrum system (Caliper Life Sciences). Recipient mice were anesthetized with isoflurane and injected intraperitoneally with D-Luciferin (200 mg/kg body weight). Mice were imaged before surgery (baseline scan) and after surgery on day 3, week 1, week 2, week 4, week 6, and week 8. Peak signals from a fixed region of interest (ROI) were evaluated and signals expressed as photons per second per centimeter square per steradian (p/sec/cm^2/sr) as described11.

Histological examination

Following imaging, mice were sacrificed and left ventricular (LV) tissue was obtained at 8 weeks after MI. Tissue samples were embedded into OCT compound (Miles Scientific). Frozen sections (5 μm thick) were processed for immunostaining. Trichrome stain (Masson, Sigma) was used to determine collagen content of the infarct regions. For each heart, eight to ten sections from apex to base (1.2 mm apart) were analyzed. Images were taken for each section to calculate the fibrotic and non-fibrotic areas as well as ventricular and septal wall thickness. Infarct fraction was determined as fibrotic area / (fibrotic + nonfibrotic area) as previously described9. To detect microvascular density (MVD) in the peri-infarct area, a rat anti-CD31 (BD Pharmingen) was used. The number of capillary vessels was counted by a blinded investigator (ZJ) in ten randomly selected areas using the picture under a fluorescent microscope, as described previously.9 The formalin-fixed and paraffin-embedded explanted hearts were used for TUNEL assay. Nuclei undergoing apoptosis were stained with DeadEnd™ Fluorometric TUNEL System (Promega) and the TUNEL positive nuclei were counted and calculated as a percentage of all nuclei according to the manufacturer's protocol. A subset of the mice (n = 3 per group) were sacrificed and the peri-infarct region of the left ventricle was dissected under stereoscope for Western blot analysis of Efna3 and Ptp1b.

Target confirmation by immuno-precipitation of c-myc-Ago2-containing RNA-induced silencing complex (RISC)

Transient miR-210 over-expression was obtained by transfection of pSUPER-pre-miR-210 using Fugene6 (Roche) in HEK-239 cells (ATCC)12. Transfected cells were harvested in 1 ml per 15 dish of cold lysis buffer supplemented with 5 mM dithiothreitol, 1 mM phenylmethylsulfonyl fluoride, protease inhibitors mixture tablets (Roche), and 100 u/ml of RNasin Plus (Promega). After 30 min at 4°C, samples were pre-cleared by A/G-agarose beads (Santa Cruz) and spun at 4°C for 30 minutes at 20,000 g in a micro-centrifuge. Next, the lysates were incubated at 4°C with 2.5 g/plate of anti-c-myc antibody (9E10, Santa Cruz) for 3 hrs and then 50 μl/plate of A/G-agarose beads were added to each sample. After 1 hr, immuno-complexes were washed two times with lysis buffer and resuspended in 200 μl of TRIzol (Invitrogen). RNA was purified and specific mRNAs were measured by quantitative real-time PCR (qPCR). Average values of 2 genes that were RISC-associated but not miR-210 targets (B2M and RPL13) were used for normalization13.

Statistical Analysis

Statistics were calculated using SPSS 16.0 (SPSS Inc., Chicago, IL, USA). Descriptive statistics included mean and standard error. One-way ANOVA and Two-way repeated measures ANOVA with post-hoc testing were used. Student's or Welch's t-test was used depending on Levene's test on variance homogeneity. If the *P* value of Levene's test was >0.05, Student's t-test was used, or else Welch's t-test was used. Differences were considered significant at *P* values of <0.05.

RESULTS

Induction of miR-210 by hypoxia in mouse HL-1 cardiomyocytes

In order to identify potential miRNA targets in our study, we first set up miRNA expression profiling experiment. Murine HL-1 cardiomyocytes were subject to hypoxia for 48 hours. Using fluorescence-activated cell sorting (FACS), we obtained two main populations of cells, apoptotic cells and live cells. We performed miRNA microarray on these two populations of cells using the Sanger miRBase Version 13.0 miRNA expression microarrays (LC Sciences, Houston, TX). We analyzed 679 unique mature miRNAs across biological duplicates of each cell type, and found that 7 miRNAs were significantly up-regulated and 13 miRNAs were significantly down-regulated in live cells compared to apoptotic cells. In particular, miRNA-210 was up-regulated ~11-fold in live cells (Figure 1**A**). To confirm the results from miRNA microarray, we selected miR-210 and miR-1187 for real-time PCR analysis. Indeed, miR-210 was significantly up-regulated in live cells (Figure 1**B**), whereas miR-1187 was significantly up-regulated in apoptotic cells (Figure 1**C**). Mir-1187 has been found to be expressed in mouse embryo stem cells by high-throughput pyrosequencing, but its function has not been elucidated yet14. We are more interested, however, in miR-210 because it has been shown to be associated with the angiogenesis associated factor and anti-apoptotic gene6, 15. To further assess whether hypoxia regulates miR-210 expression in cardiomyocytes, we also explored the time-course regulation of miR-210 in HL-1 cells. Induction of miR-210 by hypoxia was discernible at 12 hours of hypoxia, became statistically significant at 24 hours, and increased progressively to ~7-fold higher expression by 72 hours (Figure 1**D**).

Evaluation of miR-210 pro-angiogenic and anti-apoptotic functions in cardiomyocytes

To assess angiogenic potential of miR-210, HL-1 cells were transduced by a lentivirus carrying miR-210 precursor (Pre-210) or by a lentivirus carrying miR-scramble (Pre-Scr). Under fluorescence microscopy, nearly all the HL-1 cells were GFP positive in both groups, indicating no significant difference in transduction efficiency (Supplemental Figure 2). Using real-time PCR analysis, miR-210 expression was 124±15 folds higher in Pre-210 group compared to Pre-Scr group. Figure 2**A** shows that HL-1 transduced with miR-210 could release several angiogenic factors compared to control cells, including Leptin16, interleukin 1 alpha (IL-1a)17, and tumor necrosis factor alpha (Tnfα).18 In addition, Pre-210 reduced caspase 3/7 activity in HL-1 cells compared to Pre-Scr control under both normoxia (1,505,884±84,802 vs. 649,933±32,309; $P<0.01$) and hypoxia (2,832,896±97,509 vs. 1,886,473±48,009; $P<0.01$) conditions. Conversely, inhibition of miR-210 (anti-210) increased caspase 3/7 activity compared to control anti-Scr in both normoxia and hypoxia conditions (Figure 2**B**). Moreover, FACS analysis showed fewer apoptotic cells (22.13±0.48% vs 32.14±1.52%; $P<0.05$) and more live cells (71.95±1.69% vs 63.39±0.95%; $P<0.05$) in the Pre-210 group compared to Pre-Scr group after 48 hours of hypoxia stress (Figure 2**C**). Taken together, these data demonstrate miR-210 can promote angiogenesis and inhibit apoptosis.

Improvement of cardiac function following MI after injection of miR-210

To examine whether miR-210 delivery can improve cardiac function following myocardial infarction, non-viral minicircles were used to carry the miR-210 expression cassette (MC-210). As novel non-viral vectors, minicircles lack both an origin of replication and the antibiotic selection marker, and carry only short bacterial sequences. Their smaller size confers greater transfection efficiency and the lack of bacterial backbone creates less immunogenicity and longer transgene expression. We first transfected HL-1 cells with different quantities of minicircles carrying Fluc-eGFP (MC-LG) in 6-well plate (Figure 3**A**). Data showed bioluminescence signals correlated robustly with *in vitro* Fluc enzyme activity (r^2=0.96) (Figure 3**B**). Next, to monitor the duration of transgene expression mediated by MC vector in living animals, a subset of animals with LAD ligation (n=5) were injected with 25 μg of MC-LG into the heart. *In vivo* bioluminescence imaging indicated that minicircle vector-mediated gene expression was stable for at least 8 weeks in the animal heart (Figure 3**C** and 3**D**). To examine whether MC-210 can improve cardiac function, adult FVB mice underwent LAD ligation and were injected intramyocardially with *(1)* MC- 210, *(2)* MC-Scr (control), and *(3)* sham operated animals (n=15 per group). Echocardiography was performed before and after (week 2, week 4, and week 8) the LAD ligation. At baseline, left ventricular FS was comparable in all three groups (Figure 4**A**, 4**B** and Supplemental Table 1). Following LAD ligation, the MC-210 group had significantly higher left ventricular FS compared to the MC-Scr group at week 4 (28.7±2.4 vs 25.1±1.9%; P<0.05) and week 8 (27.8±1.9% vs 24.2±2.7%; P<0.05). This finding was further corroborated using invasive PV loops. The PV loop data showed that left ventricular end-diastolic volume and end-systolic volume in the MC-210 group were significantly lower than MC-Scr group, suggesting more favorable LV remodeling process after miR-210 treatment (Supplemental Table 2).

Ex vivo histological confirmation of echocardiographic data

After imaging, animals were sacrificed and hearts explanted. Masson trichrome staining showed less infarction size for the MC-210 group compared with the MC-Scr group at week 8 (Figure 4**C**), confirming the positive functional data seen in echocardiography. Calculated infarct fractions were significantly smaller in the MC-210 group compared to the MC-Scr group (26.5±2.4% vs 35.4±1.8%; P<0.05). TUNEL staining demonstrated significantly reduced apoptotic cells in the MC-210 group compared to MC-Scr group (0.13±0.01% vs 0.22±0.04%; P<0.05), whereas few or no TUNEL-positive cells could be detected in the sham group (0.009±0.003%) (Figure 4**D**). Finally, capillary status was evaluated by CD31 immunostaining in the peri-infarct areas (Figure 4**E**). Capillary density was significantly increased in the MC-210 group compared to the MC-Scr group after MI (362±25 vs 253±37 vessels/mm^2, P<0.05).

Prediction and confirmation of target genes of miR-210

To investigate the mechanism(s) of miR-210 based therapy, we predicted the target genes for miR-210 using both TargetScan and MicroCosm algorithms. Efna3, Dapk1, and Ctgf were predicted to be the putative target genes of miR-210 with high scores. The 3′-UTR segment of these three genes containing miR-210 putative binding site (“seed” sequence), which has a crucial role in miRNA:mRNA interaction, were very conserved in different species. Although it was reported that Ptp1b should be one of the miR-210 targets, the binding site was not in the 3'-UTR segment.13 To confirm that they are indeed the target genes of miR-210, the putative binding site of these target genes (Efna3, Ptp1b, Dapk1, and Ctgf) was amplified by PCR from mouse cDNA and inserted downstream of the luciferase reporter gene in the pGL3 control vector for dual-luciferase assay (Supplemental Figure 3). After NIH/3T3 cells were co-transduced with reconstructive vectors and normalizing vector pRL-TK containing Renilla luciferase, the precursor miR-210 mimic (Pre-210) significantly

reduced the luciferase activities of the wild-type Efna3, Ptp1b, Dapk1, and Ctgf reporters by 35%–60% ($P<0.05$) compared to the miR-scramble (Pre-Scr) control (Figure 5**A**). In contrast, mutant reporters with 4 nucleotides mismatching non-complementary seed binding sites were not repressed by miR-210 precursor, confirming that the target site directly mediates repression of the luciferase activity through seed specific binding. Taken together, these results demonstrate that Efna3, Ptp1b, Dapk1, and Ctgf are the target genes of miR-210.

In order to further demonstrate that they are direct miR-210 targets, biochemical assay based on the immuno-precipitation of RISC complexes enriched for miR-210 and its targets was used.13 To this end, a c-myc-tagged allele of Ago2, a core component of the RISC complex was used. Easily transfectable HEK-293 cells were co-transfected with expression vectors for miR-210 and c-myc-Ago2, yielding cells enriched of miR-210/c-myc-Ago2-containing RISC complexes as well as miR-210 targets. We then immuno-precipitated c-myc-Ago2 and measured the levels of co-immuno-precipitated mRNAs by qPCR. Background controls were represented by c-myc-immuno-precipitates derived from cells transfected with miR-210, but not c-myc-Ago2 and displayed low-to-undetectable signals for all the assayed genes (data not shown). Two known miR-210 targets (Efna3 and Ptpt1) were used as positive controls12, 19. Figure 5**B** shows that Efna3, Ptp1b, Dapk1, and Ctgf were significantly enriched in immuno-precipitates of miR-210 over-expressing cells compared to cells transfected with a scramble sequence (Pre-Scr). We concluded that Efna3, Ptp1b, Dapk1, and Ctgf are all associated with miR-210 loaded RISC complexes and hence they are the real targets of miR-210.

Endogenous regulation of Efna3 and Ptp1b by miR-210

Although these genes were identified as target genes for miR-210, it is still unknown whether miR-210 could regulate their expression endogenously. Because Efna3 and Ptp1b are involved in vascular remodeling and apoptosis in heart, respectively, we selected these two genes for confirmation in HL-1 cells. HL-1 cells were transduced with Pre-210 to assess whether miR-210 could regulate endogenous Efna3 and Ptp1b. Compared to control, the level of Efna3 mRNA was significantly down-regulated by Pre-210 (Figure 6**A**), but not Ptp1b. However, we found the level of Ptp1b protein was down-regulated on the Western blot (Figure 6**B**). These data suggest that endogenous Efna3 and Ptp1b are regulated by miR-210 at the level of mRNA and protein, respectively. Our data were also confirmed by immunofluorescence staining (Figure 6**C**). Furthermore, we also evaluated if miR-210 treatment in the heart would have an effect on Efna3 and Ptp1b. Western blot data from the peri-infarct regions of explanted hearts showed that Efna3 and Ptp1b in the MC-210 group are lower than MC-Scr group (Figure 6**D**). Taken together, these results suggest that overexpression of miR-210 led to downregulation of Efna3 on the mRNA level and downregulation of Ptp1b on the protein level. Efna3 is involved in *inhibition* of angiogenesis12, whereas Ptp1b is involved in *induction* of apoptosis.20 Therefore, the suppression of these two targets by miR-210 delivery may contribute to the improvement of cardiac function following MI.

DISCUSSION

IHD is the leading cause of human morbidity and mortality in the western world, underscoring the need for innovative new therapies for heart disease. miRNAs are 21–23 nt non-coding small RNAs that act as negative regulators of protein-coding gene by modulating the mRNA translation and stability.1, 2 In this study, we report a novel therapeutic strategy for treatment of myocardial infarction based on miR-210. Using miRNA microarray analysis, we found that miR-210 was up-regulated in live HL-1 cells compared to apoptotic cells after 48 hours of hypoxia challenge, suggesting that miR-210 possesses

anti-apoptotic properties during cell stress conditions. These data are also confirmed by a recent report indicating that miR-210 is induced in ischemia-preconditioned bone marrow derived mesenchymal stem cells and that its suppression abolished the protective effects of preconditioning due to the abnormal expression of its target FLASH/caspase-8 associated protein-2 (CASPAP2), which can activate caspase 8 and facilitate apoptosis.15

We also explored the time-course regulation of miR-210. Induction of miR-210 was discernible after 12 hours of hypoxia, and the up-regulation was maintained for the next 72 hours. This predominant induction of miR-210 by hypoxia is consistent with reports involving other cell types such as embryo kidney cells, endothelial cells, breast carcinoma cells, colonic adenocarcinoma cells, and epithelial ovarian cells.7, 12, 21 The robust induction among various cell types is probably due to the highly conserved structure of hypoxia response element (HRE) existing in miR-210 promoter.7 Under the diminished oxygen concentration of hypoxia, a variety of complex responses at both cellular and organism levels are activated, including endothelial cells proliferation, migration, and angiogenesis. The multiple lines of evidence prompted us to assess whether miR-210 delivery *in vivo* can improve heart function in a murine MI model.

Besides the therapeutic gene, the success of cardiovascular gene therapy also depends on effective delivery systems to target sites. Here we employed a non-viral minicircle vector carrying miRNA because of its multiple advantages, including greater transfection efficiency (compared to regular plasmids) and less immunogenicity (compared to viral vectors).9 miR-210 delivery through the minicircle vector improved left ventricular function after MI, and *ex vivo* histological analysis indicated that miR-210 induced neovascularization and inhibited apoptosis in ischemic hearts. Interestingly, previous studies have shown that miR-210 can improve tubulogenesis12 and prevent mesenchymal stem cell apoptosis.15 A recent study also reported that miR-210 can modulate mitochondrial respiration, iron metabolism, and ROS generation during hypoxia by repressing iron-sulfur cluster assembly proteins (ISCU1/2) to influence cellular adaptation to hypoxia, accounting for its benefits in ischemia.22 Therefore, miR-210 delivery following MI may have several pleiotropic effects in addition to the pro-angiogenesis and anti-apoptosis roles that were investigated here.

To study the potential molecular mechanism of miR-210 therapy in the heart, we performed an *in silico* search of potential targets using TargetScan and MicroCosm algorithms. We found several potential target genes for miR-210 after myocardial infarction, including Efan3, Ptp1b, Dapk1, and Ctgf. Luciferase activities of these 4 putative wild-type target genes were down-regulated by the miR-210 precursor (Pre-210), but not in mutant target sequences, suggesting that they are the real targets of miR-210 and that the inhibition was “seed” sequence specific. Efna3 and Ptp1b are involved in inhibition of angiogenesis and induction of apoptosis, respectively. Efna3 suppression in HUVEC cells is vital for stimulation of tubulogenesis, indicating its crucial function in angiogenesis.12 Ppt1b is an ubiquitously expressed 50-Kda enzyme that is the most widely studied prototype for the protein tyrosine phosphatase (PTP) superfamily. Recently, it has been reported that Ptp1b inhibition by siRNA significantly decreased apoptosis in cardiomyocyte.20 Ppt1b has also been implicated as a negative regulator in VEGF signaling in endothelial cells.23 Dapk1, which encodes a proapoptotic serine/threonine kinase, is critical for regulating the cell cycle, apoptosis, and metastasis, mainly functioning in the early stages of eukaryotic programmed cell death.24 Connective tissue growth factor (Ctgf) is a secreted cysteine-rich protein with major roles in angiogenesis, chondrogenesis, osteogenesis, tissue repair, cancer, and fibrosis. Ctgf expression is enhanced in cardiac myocytes and fibroblasts in the heart after myocardial infarction25 and is induced by TGF-β in heart fibrosis.26 Thus, the inhibition by miR-210 delivery after MI may favor the functional improvement of left ventricle through

direct inhibition of these target genes, especially Efna3 and Ptp1b as investigated in this study.

In conclusion, we found that miR-210 can improve heart function by up-regulating angiogenesis and inhibiting apoptosis. Because individual miRNAs can regulate the expression of multiple target genes, manipulating miRNA expression can influence an entire gene network and thereby modify complex disease pathology. Our approach shows that miR-210 delivery via non-viral minicircle may work as a novel therapeutic avenue for treatment of IHD.

Supplementary Material

Refer to Web version on PubMed Central for supplementary material.

Acknowledgments

We thank Dr. Jarrett Rosenberg for assistance in biostatistical analysis.

Funding: This work was supported in part by grants from the NIH HL093172, NIH HL095571, Baxter Faculty Scholar Award (JCW), and Italian Ministry of Health (Ministero della Salute) (FM).

REFERENCES

1. Bartel DP. MicroRNAs: genomics, biogenesis, mechanism, and function. Cell. 2004; 116:281–297. [PubMed: 14744438]
2. Filipowicz W, Bhattacharyya SN, Sonenberg N. Mechanisms of post-transcriptional regulation by microRNAs: are the answers in sight? Nat Rev Genet. 2008; 9:102–114. [PubMed: 18197166]
3. Kota J, Chivukula RR, O'Donnell KA, Wentzel EA, Montgomery CL, Hwang HW, Chang TC, Vivekanandan P, Torbenson M, Clark KR, Mendell JR, Mendell JT. Therapeutic microRNA delivery suppresses tumorigenesis in a murine liver cancer model. Cell. 2009; 137:1005–1017. [PubMed: 19524505]
4. Barringhaus KG, Zamore PD. MicroRNAs: regulating a change of heart. Circulation. 2009; 119:2217–2224. [PubMed: 19398677]
5. Dong S, Cheng Y, Yang J, Li J, Liu X, Wang X, Wang D, Krall TJ, Delphin ES, Zhang C. MicroRNA expression signature and the role of microRNA-21 in the early phase of acute myocardial infarction. J Biol Chem. 2009; 284:29514–29525. [PubMed: 19706597]
6. Ivan M, Harris AL, Martelli F, Kulshreshtha R. Hypoxia response and microRNAs: no longer two separate worlds. J Cell Mol Med. 2008; 12:1426–1431. [PubMed: 18624759]
7. Huang X, Ding L, Bennewith KL, Tong RT, Welford SM, Ang KK, Story M, Le QT, Giaccia AJ. Hypoxia-inducible mir-210 regulates normoxic gene expression involved in tumor initiation. Mol Cell. 2009; 35:856–867. [PubMed: 19782034]
8. Tiscornia G, Singer O, Verma IM. Production and purification of lentiviral vectors. Nat Protoc. 2006; 1:241–245. [PubMed: 17406239]
9. Huang M, Chen Z, Hu S, Jia F, Li Z, Hoyt G, Robbins RC, Kay MA, Wu JC. Novel minicircle vector for gene therapy in murine myocardial infarction. Circulation. 2009; 120(11 Suppl):S230–S237. [PubMed: 19752373]
10. Li Z, Lee A, Huang M, Chun H, Chung J, Chu P, Hoyt G, Yang P, Rosenberg J, Robbins RC, Wu JC. Imaging survival and function of transplanted cardiac resident stem cells. J Am Coll Cardiol. 2009; 53:1229–1240. [PubMed: 19341866]
11. Cao F, Lin S, Xie X, Ray P, Patel M, Zhang X, Drukker M, Dylla SJ, Connolly AJ, Chen X, Weissman IL, Gambhir SS, Wu JC. In vivo visualization of embryonic stem cell survival, proliferation, and migration after cardiac delivery. Circulation. 2006; 113:1005–1014. [PubMed: 16476845]
12. Fasanaro P, D'Alessandra Y, Di Stefano V, Melchionna R, Romani S, Pompilio G, Capogrossi MC, Martelli F. MicroRNA-210 modulates endothelial cell response to hypoxia and inhibits the

receptor tyrosine kinase ligand Ephrin-A3. J Biol Chem. 2008; 283:15878–15883. [PubMed: 18417479]

13. Fasanaro P, Greco S, Lorenzi M, Pescatori M, Brioschi M, Kulshreshtha R, Banfi C, Stubbs A, Calin GA, Ivan M, Capogrossi MC, Martelli F. An integrated approach for experimental target identification of hypoxia-induced miR-210. J Biol Chem. 2009
14. Calabrese JM, Seila AC, Yeo GW, Sharp PA. RNA sequence analysis defines Dicer's role in mouse embryonic stem cells. Proc Natl Acad Sci U S A. 2007; 104:18097–18102. [PubMed: 17989215]
15. Kim HW, Haider HK, Jiang S, Ashraf M. Ischemic preconditioning augments survival of stem cells via MIR-210 expression by targeting caspase-8 associated protein 2. J Biol Chem. 2009; 284:33161–33168. [PubMed: 19721136]
16. Hausman GJ, Richardson RL. Adipose tissue angiogenesis. J Anim Sci. 2004; 82:925–934. [PubMed: 15032451]
17. Bando Y, Noguchi K, Kobayashi H, Yoshida N, Ishikawa I, Izumi Y. Cyclooxygenase-2-derived prostaglandin E2 is involved in vascular endothelial growth factor production in interleukin-1alpha-stimulated human periodontal ligament cells. J Periodontal Res. 2009; 44:395–401. [PubMed: 19210337]
18. Ferrara N. Vascular endothelial growth factor as a target for anticancer therapy. Oncologist. 2004; 9 Suppl 1:2–10. [PubMed: 15178810]
19. Silvestri P, Di Russo C, Rigattieri S, Fedele S, Todaro D, Ferraiuolo G, Altamura G, Loschiavo P. MicroRNAs and ischemic heart disease: towards a better comprehension of pathogenesis, new diagnostic tools and new therapeutic targets. Recent Pat Cardiovasc Drug Discov. 2009; 4:109–118. [PubMed: 19519553]
20. Song H, Zhang Z, Wang L. Small interference RNA against PTP-1B reduces hypoxia/reoxygenation induced apoptosis of rat cardiomyocytes. Apoptosis. 2008; 13:383–393. [PubMed: 18278556]
21. Giannakakis A, Sandaltzopoulos R, Greshock J, Liang S, Huang J, Hasegawa K, Li C, O'Brien-Jenkins A, Katsaros D, Weber BL, Simon C, Coukos G, Zhang L. miR-210 links hypoxia with cell cycle regulation and is deleted in human epithelial ovarian cancer. Cancer Biol Ther. 2008; 7:255–264. [PubMed: 18059191]
22. Chan SY, Zhang YY, Hemann C, Mahoney CE, Zweier JL, Loscalzo J. MicroRNA-210 controls mitochondrial metabolism during hypoxia by repressing the iron-sulfur cluster assembly proteins ISCU1/2. Cell Metab. 2009; 10:273–284. [PubMed: 19808020]
23. Nakamura Y, Patrushev N, Inomata H, Mehta D, Urao N, Kim HW, Razvi M, Kini V, Mahadev K, Goldstein BJ, McKinney R, Fukai T, Ushio-Fukai M. Role of protein tyrosine phosphatase 1B in vascular endothelial growth factor signaling and cell-cell adhesions in endothelial cells. Circ Res. 2008; 102:1182–1191. [PubMed: 18451337]
24. Maiuri MC, Tasdemir E, Criollo A, Morselli E, Vicencio JM, Carnuccio R, Kroemer G. Control of autophagy by oncogenes and tumor suppressor genes. Cell Death Differ. 2009; 16:87–93. [PubMed: 18806760]
25. Ohnishi H, Oka T, Kusachi S, Nakanishi T, Takeda K, Nakahama M, Doi M, Murakami T, Ninomiya Y, Takigawa M, Takigawa M, Tsuji T. Increased expression of connective tissue growth factor in the infarct zone of experimentally induced myocardial infarction in rats. J Mol Cell Cardiol. 1998; 30:2411–2422. [PubMed: 9925376]
26. Chen MM, Lam A, Abraham JA, Schreiner GF, Joly AH. CTGF expression is induced by TGF-beta in cardiac fibroblasts and cardiac myocytes: a potential role in heart fibrosis. J Mol Cell Cardiol. 2000; 32(10):1805–1819. [PubMed: 11013125]

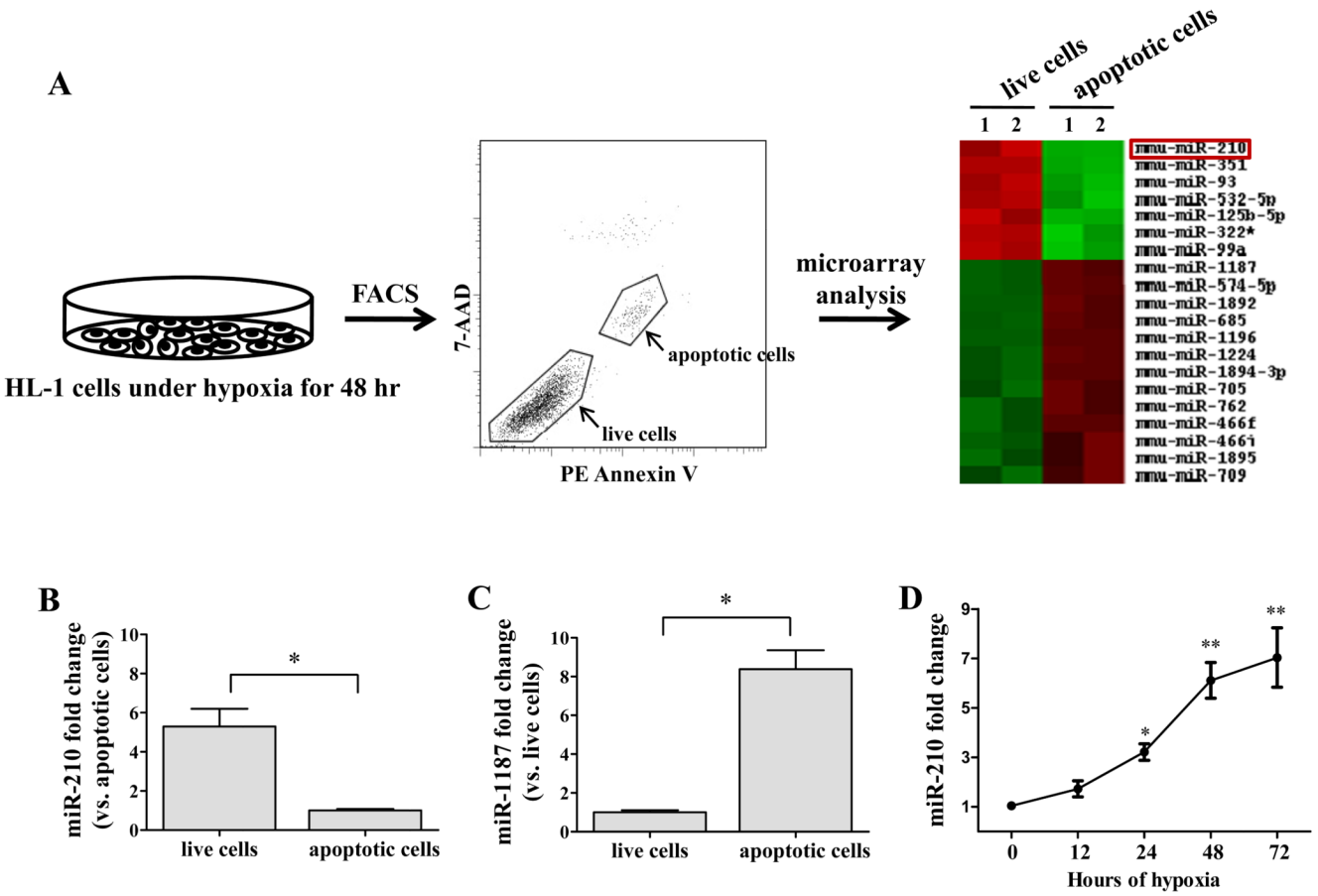

Figure 1.

(A) Schematic highlighting the microRNA microarray experimental design. HL-1 cells were subjected to hypoxia for 48 hours. Following FACS, apoptotic cells and live cells were collected for miRNA microarray analysis. T-test analysis demonstrates statistically significant differential miRNA expression across the two samples. miRNAs with $P<0.05$ were selected for cluster analysis. (B) Quantitative RT-PCR showed miR-210 expression was 5.3±0.9 fold higher in live cells than in apoptotic cells. Welch's t-test was used. (C) Quantitative RT-PCR showed miR-1187 expression was 8.4±0.9 folds higher in apoptotic cells compared to in live cells. Welch's t-test was used. (D) Time course regulation of miR-210 by hypoxia in HL-1 cells. Induction of miR-210 was discernible at 12 hours, becoming significant at 24 hours and increased progressively at 48 and 72 hour time points. 1-way ANOVA was used. *$P<0.01$ and **$P<0.05$.

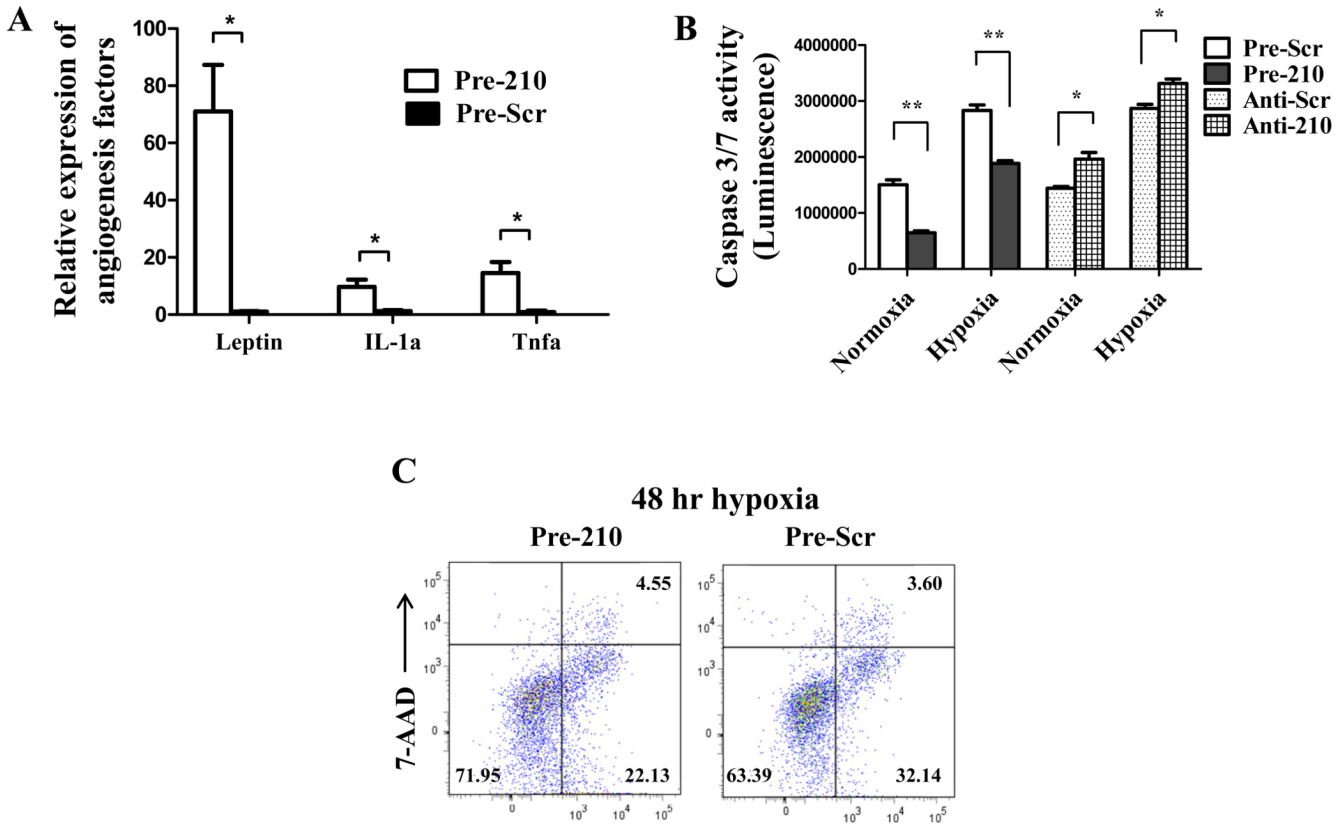

Figure 2.

In vitro characterization of therapeutic potential for miR-210. (A) Angiogenesis antibody array indicated miR-210 can release several angiogenic factors in HL-1 cells. Welch's t-test was used for statistical analysis. (B) Caspase 3/7 activity assay demonstrated that miR-210 overexpression could inhibit caspase activity whereas inhibition of miR-210 with anti-210 abrogated the favorable effect. Student's t-test was used. (C) FACS analysis confirmed that miR-210 transduced group had more live cells (71.95±1.69% vs 63.39±0.95%; $P<0.05$) and less apoptotic cells (22.13±0.48% vs 32.14±1.52%; $P<0.05$). Student's t-test was used. *$P<0.01$ and **$P<0.05$.

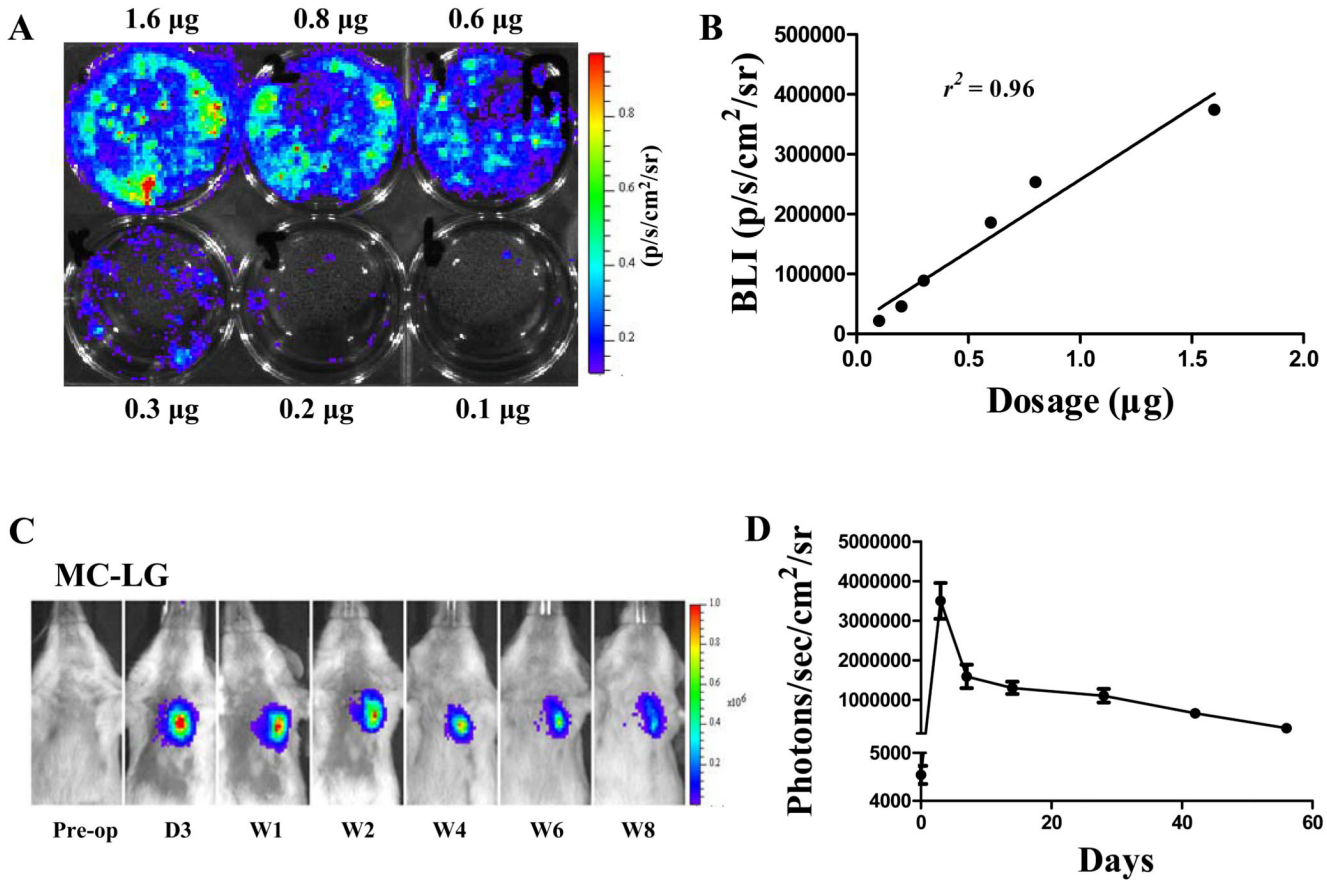

Figure 3.

Transfection efficiency of minicircle *in vitro* and *in vivo*. (A) HL-1 cells were transfected with MC-Fluc-eGFP (MC-LG) in 6-well plate. (B) A robust correlation exists between minicircle dosage and bioluminescence signals (r^2=0.96). Each data point is from an individual observation. Pearson's correlation was used. (C) Bioluminescence imaging and (D) quantitative analysis indicate minicircle plasmid-mediated gene expression was stable for at least 8 weeks in the heart compared to <4 weeks using regular plasmid (data not shown).

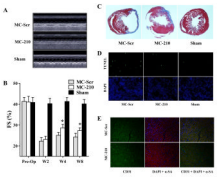

Figure 4.

Evaluation of cardiac function following MI after miR-210 treatment. (A) Representative echocardiogram of mice with LAD ligation after injection of MC-210, MC-Scr, or sham group at week 8. (B) Quantitative analysis of left ventricular fractional shortening (FS) among the 3 groups. Compared to MC-Scr control, animals injected with MC-210 had significant improvements in FS values at both week 4 and week 8. 2-way ANOVA was used for statistical analysis. (C) Representative Masson trichrome staining of explanted heart at week 8 showed increased wall thickness for the MC-210 group, confirming the positive functional imaging data seen in echocardiography. (D) TUNEL staining of explanted heart demonstrated significantly reduced apoptotic cells in MC-210 group compared to MC-Scr control group. (E) Immunofluorescence staining of CD31 endothelial marker (green) demonstrated increased neovascularization in the myocardium after MC-210 delivery compared to MC-Scr control. Cardiomyocyte staining is identified by α-sarcomeric actin (red) and nuclear staining is identified by DAPI (blue).

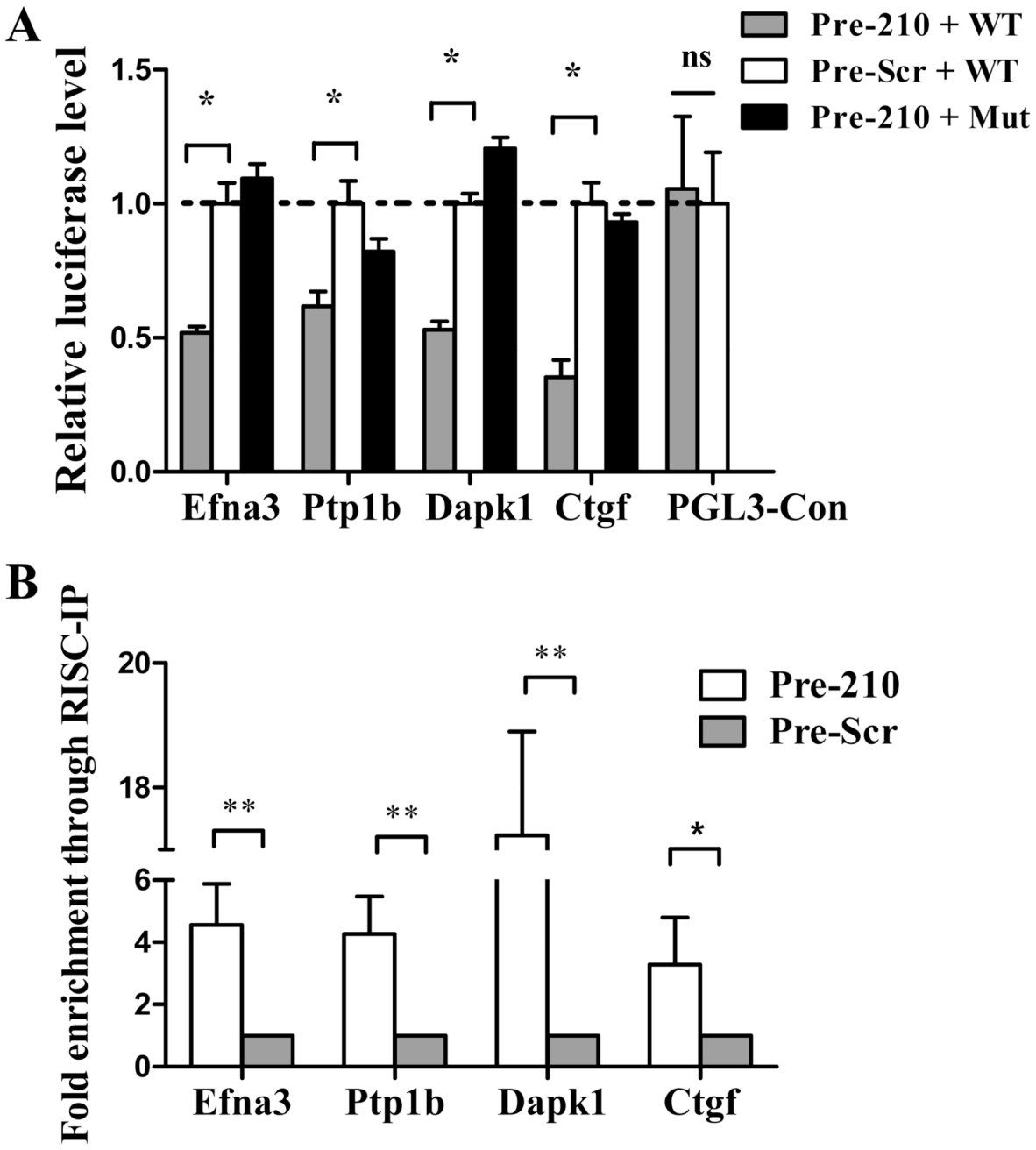

Figure 5.

Confirmation of the target gene of miR-210. (A) The binding segments of mouse Efna3, Ptp1b, Dapk1, and Ctgf interacting with miR-210 was amplified and inserted downstream of firefly luciferase reporter gene in the pGL3 control vector for dual-luciferase assay (see Supplemental Figure 3). pRL-TK containing renilla luciferase was co-transfected for data normalization. Precursor miR-210 mimic (Pre-210) significantly reduced the luciferase activities of the wild-type Efna3, Ptp1b, Dapk1, and Ctgf reporters between 35%–60% compared to the Pre-miR scramble control (Pre-Scr). However, mutant reporters (Pre-210 + Mut) with non-complementary seed binding site were not repressed by miR-210 precursor as expected. The blank vector (PGL3-control) has no seed binding site and therefore the

firefly luciferase activity was not affected by miR-210 precursor mimic. 1-way ANOVA was used. (B) miR-210 targets were enriched in miR-210 containing RISC. Compared to cells transfected with a scramble sequence, immune-precipitates of the miR-210 loaded RISC highly enriched its targets, including Efna3, Ptp1b, Dapk1, and Ctgf. Student's t-test was used. *P<0.05 and **P<0.01.

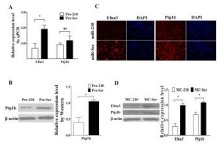

Figure 6.

Endogenous regulation of Efna3 and Ptp1b by miR-210. (A) Quantitative RT-PCR indicate miR-210 can inhibit Efna3 but not Ptp1b at the RNA level. Student's t-test was used. (B) However, Western blotting showed Ptp1b can be inhibited at the protein level instead. Student's t-test was used. (C) Immunofluorescence confirmed miR-210 can strongly diminish Efna3 and Ptp1b expression in HL-1 cardiomyocytes. (D) Western blot data show that Efnas and Ptp1b from the peri-infarct regions of explanted hearts are significantly lower in the MC-210 group compared to MC-Scr group. Student's t-test was used. **P*<0.05.